Journal of
Functional Biomaterials

MDPI

Article

Effect of Hydrothermal Aging on Translucency, Phase Transformation, and Mechanical Properties of Multilayer Monolithic Zirconia Materials

Murat Alkurt * and Mamasaly Abdinabi Uulu

Department of Prosthodontics, Faculty of Dentistry, Recep Tayyip Erdoğan University, Rize 53100, Türkiye
* Correspondence: murat.alkurt@erdogan.edu.tr; Tel.: +90-545-878-81-63; Fax: + 90-464-222-0002

Abstract

Background/Objectives: This in-vitro study aimed to evaluate the effects of hydrothermal aging on translucency, phase transformation, surface topography, surface hardness, and biaxial flexural strength. Methods: Three multilayered zirconia materials (Katana Zirconia, Kuraray Noritake), namely Ultra Translucent Multi-Layered (UTML), Super Translucent Multi-Layered (STML), and Multi-Layered (ML), were evaluated. Each material was divided into control, 5-h, and 10-h hydrothermal aging groups. A total of 81 specimens ($n = 9$ per subgroup) were evaluated. The specimens were evaluated using spectrophotometry, XRD, SEM, Vickers hardness, and biaxial flexural strength tests. Data were analyzed using two-way ANOVA and three-way mixed-design ANOVA, followed by Tukey's post-hoc test ($\alpha = 0.05$). Results: Material type ($p < 0.001$), hydrothermal aging duration ($p = 0.023$), and measurement time ($p < 0.001$) significantly affected translucency. A significant interaction between aging duration and measurement time was also observed ($p = 0.002$), with a greater reduction in TP after 10 h than after 5 h of aging. Hydrothermal aging did not significantly affect Vickers hardness ($p > 0.05$), whereas material type had a significant effect ($p < 0.05$), with UTML exhibiting significantly higher hardness than ML. Hydrothermal aging increased the monoclinic phase content in all materials, with ML showing the greatest transformation. Biaxial flexural strength was significantly affected by material type and aging duration ($p < 0.05$), with ML exhibiting the highest strength and an overall increase following aging. Conclusions: Hydrothermal aging significantly reduced the translucency of the multilayered zirconia materials. Phase transformation was more pronounced in ML than in UTML and STML. ML exhibited the highest biaxial flexural strength, whereas UTML showed the lowest. Overall, hydrothermal aging increased biaxial flexural strength, although the response varied among materials.

Keywords: monolithic zirconia; low-temperature degradation; hydrothermal aging; translucency; phase transformation; biaxial flexural strength; vickers hardness

Check for updates

Academic Editors: Tareq Hajaj, Ioana Veja and Mihai Rominu

Received: 22 October 2026
Revised: 7 November 2026
Accepted: 10 November 2026
Published: 12 November 2026

Copyright: © 2026 by the authors. Licensee MDPI, Basel, Switzerland. This article is an open access article distributed under the terms and conditions of the Creative Commons Attribution (CC BY) license.

1. Introduction

Zirconia has become a widely used material for full-contour monolithic restorations due to its superior mechanical properties compared with other dental ceramic systems. In addition to its high mechanical performance, zirconia exhibits favorable esthetic properties, biocompatibility, radiopacity, chemical stability, low corrosion potential, and dimensional stability, making it a suitable material for a wide range of clinical applications [1–3]. Among zirconia-based ceramics, yttria-stabilized tetragonal zirconia polycrystal (Y-TZP) has been

widely used in dentistry because the addition of yttria stabilizes the tetragonal phase at room temperature and contributes to its favorable mechanical properties [2]. Traditionally, Y-TZP was used as a framework material veneered with translucent feldspathic porcelain to fabricate bilayered zirconia restorations [4]. However, chipping of the porcelain veneer is one of the most frequent complications associated with bilayered zirconia restorations, leading to a shift toward monolithic zirconia restorations [5,6]. Recently developed translucent monolithic zirconia materials provide improved optical properties while maintaining mechanical performance suitable for a wide range of anterior and posterior restorations [7]. Compared with conventional 3 mol% yttria-stabilized tetragonal zirconia polycrystal (3Y-TZP), newer generations containing approximately 4 and 5 mol% yttria (4Y-PSZ and 5Y-PSZ) have been developed to improve translucency by modifying their phase composition and microstructure [8]. Increasing the yttria content generally increases the proportion of optically favorable phases and improves translucency; however, this improvement may be accompanied by a reduction in transformation toughening and flexural strength, resulting in a trade-off between optical and mechanical properties [8].

Y-TZP can undergo a tetragonal-to-monoclinic (t→ m) phase transformation under mechanical stress, accompanied by a local volume expansion that generates compressive stresses around crack tips and thereby contributes to crack resistance [9,10]. However, the tetragonal-to-monoclinic transformation may also occur spontaneously during exposure to moisture at relatively low temperatures, a phenomenon known as low-temperature degradation (LTD) or hydrothermal aging [10,11]. The susceptibility of dental zirconia to LTD is influenced by several material- and processing-related factors, including yttria content, grain size, residual stresses, surface treatment, and sintering conditions [12]. Current evidence indicates that susceptibility to hydrothermal degradation differs among zirconia generations, with predominantly tetragonal zirconia showing greater t→ m transformation, whereas zirconia with a higher content of transformation-resistant phases generally exhibits greater phase stability during aging [13]. As the phase transformation progresses, intergranular microcracks may develop, potentially compromising the mechanical integrity of the material [14]. To improve phase stability and reduce spontaneous t→ m transformation, stabilizing oxides are incorporated into zirconia, with yttrium oxide (Y_2O_3) commonly used as a stabilizer in dental zirconia [15,16].

Conventional dental zirconia is predominantly based on 3 mol% yttria-stabilized tetragonal zirconia polycrystal (3Y-TZP), which provides high mechanical strength and transformation-toughening capability but has relatively limited translucency [8]. To improve optical properties, newer zirconia compositions with higher yttria contents, particularly 4Y-PSZ and 5Y-PSZ, have been developed, resulting in modifications of phase composition and microstructure that enhance translucency but may reduce mechanical strength [8]. Accelerated hydrothermal aging at 134 °C and 0.2 MPa has therefore been widely used to investigate the aging behavior of dental zirconia, with 5- and 10-h exposure periods employed to evaluate progressive changes in phase composition, surface characteristics, and mechanical properties [17].

Previous studies have reported variable effects of hydrothermal aging on translucent zirconia, particularly regarding changes in optical and mechanical properties. Although aging-induced phase transformation and changes in translucency have been widely reported, the influence of hydrothermal aging on mechanical properties remains less consistent across different zirconia compositions and aging conditions [17,18].

Accordingly, this study aimed to provide an integrated evaluation of the effects of hydrothermal aging on multilayer translucent monolithic zirconia ceramics using complementary optical, microstructural, and mechanical analyses.

The null hypothesis was that hydrothermal aging would have no significant effect on the translucency parameter (TP), phase transformation, Vickers hardness, or biaxial flexural strength of the evaluated monolithic zirconia materials.

2. Materials and Methods

2.1. Specimen Preparation

Three commercially available presintered monolithic zirconia blocks—Ultra Translucent Multi-Layered (UTML), Super Translucent Multi-Layered (STML), and Multi-Layered (ML)—from the Katana Zirconia system (Kuraray Noritake Dental Inc., Tokyo, Japan) were used in this study. The presintered zirconia blocks were 98 mm in diameter and 18 mm in thickness.

Based on the compositional analysis reported by Kolakarnprasert et al. [19], UTML, STML, and ML were classified as approximately 5Y-PSZ, 4Y-PSZ, and 3Y-PSZ, respectively. The corresponding yttria contents reported in that study were approximately 5.4, 4.8, and 3.7 mol%, respectively.

All disc-shaped specimens were positioned horizontally at the midpoint of the 18-mm-thick multilayer zirconia blanks during CAD/CAM milling, with their flat surfaces parallel to the layering planes. The same positioning and orientation were maintained for all specimens to standardize the sampling location within the multilayer structure. All measurements were performed on the same designated surface of the specimens to ensure consistency in surface orientation across the experimental groups.

Following CAD/CAM milling, the presintered zirconia specimens underwent final sintering according to the manufacturer's recommended sintering protocol.

A total of 81 disc-shaped specimens were fabricated using a CAD/CAM milling system (Redon Hybrid, Redon Technology, Istanbul, Turkey) in accordance with ISO 6872 standards [20]. The sample size calculation indicated that nine specimens per material–aging subgroup ($n = 9$) would provide adequate statistical power for the experimental design at an α level of 0.05. Following sintering, the final specimen dimensions were 15 mm in diameter and 1.2 mm in thickness. Sintering was performed according to the manufacturer's standard sintering program, using a heating rate of 10 °C/min to a final sintering temperature of 1550 °C for UTML and STML and 1500 °C for ML. The specimens were held at the final sintering temperature for 120 min, followed by controlled cooling at a rate of 10 °C/min.

Following sintering, the specimens were maintained in their as-sintered condition without additional grinding, polishing, or airborne-particle abrasion. Subsequently, the specimens were cleaned in an ultrasonic bath containing distilled water for 60 s and air-dried before testing.

2.2. Measurement of Translucency Parameters

Translucency was evaluated using a spectrophotometer (Vita EasyShade, Vita Zahnfabrik, Bad Säckingen, Germany). For the 5 h and 10 h hydrothermal aging groups, translucency measurements were performed on the same specimens before and after aging. Each sample was measured three times against black (L* = 37.4, a* = −0.5, b* = 0.6) and white (L* = 89.0, a* = 1.0, b* = 1.1) backgrounds.

A total of 54 specimens ($n = 9$ per material–aging duration subgroup) were included in the translucency analysis, with paired measurements obtained before and after hydrothermal aging.

Translucency measurements obtained before hydrothermal aging served as baseline values for each specimen. The same specimens were remeasured after 5 or 10 h of aging,

allowing paired within-specimen comparisons. Therefore, the translucency analysis focused on changes from baseline rather than comparisons with a separate non-aged control group.

The translucency parameter (TP) was calculated from the CIELAB color differences in each specimen measured against the white and black backgrounds using the following equation [21]:

$$TP = [(L^*_b - L^*_w)^2 + (a^*_b - a^*_w)^2 + (b_{*b} - b^*_w)^2]^{1/2}$$

$$(_b = \text{black background}, _w = \text{white background})$$

where the subscripts $_b$ and $_w$ represent measurements obtained against the black and white backgrounds, respectively. A TP value of 0 indicates complete opacity, whereas higher TP values indicate greater translucency [21].

2.3. Hydrothermal Aging Process

Each material group was divided into three subgroups according to the hydrothermal aging duration: control (no aging), 5 h, and 10 h. Hydrothermal aging was performed in an autoclave (Getinge GE 6610, Getinge Sterilization AB, Getinge, Sweden) using distilled water at 134 °C and 0.2 MPa, following the hydrothermal aging conditions specified in ISO 13356 [22]. This protocol was used as an accelerated hydrothermal aging method to induce low-temperature degradation. The 5- and 10-h aging periods were selected to evaluate the time-dependent progression of hydrothermal degradation and to enable comparison with previous studies using similar aging protocols [17]. Based on commonly cited theoretical estimates, 1 h of autoclave aging at 134 °C has been suggested to correspond to approximately 3–4 years of in vivo aging; therefore, 5 and 10 h may theoretically represent approximately 15–20 and 30–40 years of aging, respectively [10].

2.4. X-Ray Diffraction (XRD) Analysis

Eight specimens from each of the nine experimental subgroups were subjected to XRD analysis ($n = 8$ per subgroup; 72 specimens in total). The phase composition of the zirconia specimen surfaces was analyzed by X-ray diffraction (XRD) using an X-ray diffractometer (SmartLab, Rigaku Corporation, Akishima, Japan). XRD patterns were recorded over a 2θ range of 20–40°, with a step size of 0.02° and a counting time of 3 s per step. The relative monoclinic phase fraction (XM) was calculated from the integrated intensities of the monoclinic and tetragonal diffraction peaks using the Garvie and Nicholson method [23], as follows:

$$X_M = [\, I_M\,(-111) + I_M\,(111)]/[\, I_M\,(-111) + I_M\,(111) + I_T\,(101)]$$

where $I_M\,(-111)$ and $I_M\,(111)$ represent the integrated intensities of the monoclinic peaks at $2\theta = 28.2°$ and 31.5°, respectively, and $I_T\,(101)$ represents the integrated intensity of the tetragonal peak at $2\theta = 30°$.

2.5. Scanning Electron Microscope Analysis (SEM)

One specimen from each experimental subgroup was allocated to SEM examination ($n = 1$ per subgroup; nine specimens in total). SEM analysis was performed to evaluate surface morphology and microstructural changes in the specimens. Prior to SEM examination, the specimens were sputter-coated with a thin layer of gold using a sputter coater (SC7620, Quorum Technologies, Newhaven, UK) to provide electrical conductivity. The specimens were examined using a scanning electron microscope (JSM-6610, JEOL, Peabody, MA, USA) at an accelerating voltage of 2.0 kV. Surface morphology was documented at magnifications of ×100 and ×2000.

2.6. Vickers Surface Hardness Analysis

Vickers hardness was measured using a hardness tester (TMTeck HV, Beijing, China) under a load of 9.8 N with a dwell time of 15 s. For each specimen, three Vickers indentations were made at different locations on the surface under the specified testing conditions (Figure 1). The three indentation values were averaged to obtain one specimen-level hardness value for statistical analysis ($n = 9$ specimens per subgroup; 81 specimen-level values in total).

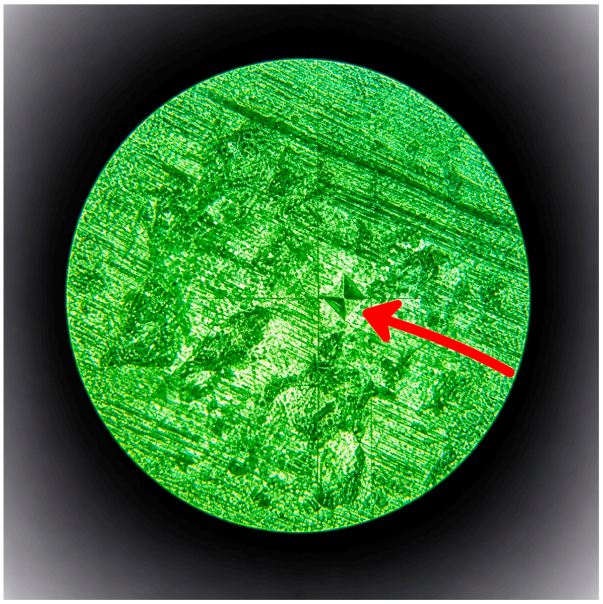


Figure 1. Microscopic image of Vickers hardness indentations. The tip of the red arrow indicates a Vickers indentation.

2.7. Biaxial Flexural Strength (BFS) Analysis

Biaxial flexural strength (BFS) testing was performed using a universal testing machine (Instron 3340, Instron, Wycombe, UK) at a crosshead speed of 1 mm/min. The maximum load at fracture was recorded in Newtons (N) and subsequently used to calculate the BFS in megapascals (MPa). The BFS test setup was configured according to ISO 6872 [20]. Three steel balls, each 3.4 mm in diameter, were positioned at equal intervals on a 10-mm-diameter support circle. Each specimen was concentrically positioned on the three supporting balls, and the load was applied to the center of the specimen using a cylindrical loading tip with a diameter of 1.4 mm.

Biaxial flexural strength was calculated according to ISO 6872 using the following equation [20]:

$S = -0.2387P\ (X - Y)/d^2$. where S is the biaxial flexural strength (MPa), P is the fracture load (N), and d is the specimen thickness (mm). The parameters X and Y were calculated as follows:

$$X = (1 + \nu)\ \ln(r_2/r_3)^2 + [(1 - \nu)/2]\ (r_2/r_3)^2$$

$$Y = (1 + \nu)\ [1 + \ln(r_1/r_3)^2] + (1 - \nu)\ (r_1/r_3)^2$$

where ν is Poisson's ratio (0.25), r_1 is the radius of the support circle, r_2 is the radius of the loaded area, and r_3 is the radius of the sample [24].

2.8. Statistical Analysis

For the TP analysis, material type (UTML, STML, and ML) and aging duration (5 h and 10 h) were considered between-subject factors, whereas measurement time (before and after

hydrothermal aging) was treated as a within-subject factor. The TP data were analyzed using a three-way mixed-design analysis of variance (ANOVA), whereas Vickers hardness, monoclinic phase fraction, and biaxial flexural strength data were analyzed using two-way ANOVA. Tukey's multiple comparison test was used for post-hoc comparisons where appropriate. TP and Vickers hardness analyses were recalculated using Python (version 3.10; Python Software Foundation, Wilmington, DE, USA) with the statsmodels library (version 0.13.5); the remaining statistical analyses were performed using IBM SPSS Statistics 20 (SPSS v20.0; SPSS Inc., Chicago, IL, USA). Statistical significance was set at $p < 0.05$.

3. Results

3.1. Translucency Parameter (TP) Values

Three-way mixed-design ANOVA revealed significant main effects of material type ($p < 0.001$), aging duration ($p = 0.023$), and measurement time ($p < 0.001$) on TP values. Among the two-way interactions, only the interaction between aging duration and measurement time was statistically significant ($p = 0.002$). The interactions between material type and measurement time ($p = 0.132$), material type and aging duration ($p = 0.150$), and the three-way interaction ($p = 0.279$) were not statistically significant (Table 1).

Table 1. Descriptive statistics and three-way mixed-design ANOVA results for the translucency parameter (TP) of monolithic zirconia materials. (**A**) Material-specific TP values and post-hoc comparisons. (**B**) ANOVA main effects and interactions. (**C**) TP values before and after hydrothermal aging.

(**A**) Overall TP values by zirconia material			
Material	Mean TP ± SD		
UTML	7.928 [a] ± 0.365		
STML	7.255 [b] ± 0.472		
ML	6.910 [b] ± 0.458		
(**B**) Three-way mixed-design ANOVA for TP			
Source of variation	df	F	*p*
Material	2.48	28.82	<0.001
Aging duration	1.48	5.55	0.023
Measurement time	1.48	133.93	<0.001
Material × Aging duration	2.48	1.97	0.150
Material × Measurement time	2.48	2.12	0.132
Aging duration × Measurement time	1.48	11.21	0.002
Material × Aging duration × Measurement time	2.48	1.31	0.279
(**C**) TP changes by aging duration			
Aging duration	Before aging	After aging	Mean change
5 h	8.004	6.987	−1.017
10 h	8.155	6.311	−1.845

Values are presented as mean ± standard deviation of specimen-level averages across measurement times. Different superscript letters indicate significant differences between materials (Tukey-adjusted $p < 0.05$); STML versus ML was not significant ($p = 0.054$). Measurement time was a within-subject factor; material and aging duration were between-subject factors. df: numerator and denominator degrees of freedom. Values are means across the three materials ($n = 27$ specimens per aging-duration group); mean change = after − before.

Tukey-adjusted pairwise comparisons showed that UTML had significantly higher TP values than STML and ML ($p < 0.001$), whereas the difference between STML and ML was not statistically significant ($p = 0.054$). UTML exhibited the highest overall mean TP value (7.928 ± 0.365), followed by STML (7.255 ± 0.472) and ML (6.910 ± 0.458).

Hydrothermal aging duration significantly affected TP values ($p = 0.023$). The overall mean TP values were 7.495 and 7.233 in the 5 h and 10 h aging groups, respectively. A significant interaction between aging duration and measurement time was observed ($p = 0.002$). The mean TP decreased from 8.004 to 6.987 in the 5 h group and from 8.155 to 6.311 in the 10 h group, indicating a greater reduction in translucency following prolonged hydrothermal aging.

3.2. Vickers Surface Hardness Values (HV)

Two-way ANOVA based on specimen-level mean Vickers hardness values ($n = 81$) revealed a significant effect of material type ($p < 0.05$), whereas hydrothermal aging duration ($p > 0.05$) and the interaction between material type and aging duration ($p > 0.05$) were not statistically significant (Table 2).

Table 2. Two-way Variance Analysis of Vickers Surface Hardness Values.

Source of Variation	Sum of Squares (SS)	Degrees of Freedom (df)	Mean Square (MS)	F	*p*
Intercept	144,060,513.023	1	144,060,513.023	2075.946	<0.001
Material	836,225.804	2	418,112.902	6.025	0.0038
Aging	40,682.654	2	20,341.327	0.293	0.7468
Material × Aging	290,310.479	4	72,577.620	1.046	0.3897
Error	4,996,447.950	72	69,395.110	—	—
Total	150,224,179.910	81	—	—	—

Tukey HSD comparisons showed significantly higher mean Vickers hardness for UTML (1469.97 ^{a} ± 310.87 HV) than for ML (1226.18 ^{b} ± 247.47 HV) ($p < 0.05$). No significant differences were observed between UTML and STML (1304.70 ^{ab} ± 216.84 HV) or between STML and ML ($p > 0.05$).

3.3. XRD Analysis

Two-way ANOVA revealed significant effects of both aging time and material type on the monoclinic phase fraction ($p < 0.05$). A significant interaction between aging time and material type was also observed ($p < 0.05$) (Table 3).

Table 3. Two-way ANOVA of Monoclinic Phase Fraction.

Source of Variation	Sum of Squares (SS)	Degrees of Freedom (df)	Mean Square (MS)	F	*p*
Intercept	0.462882	1	0.462882	2285.413	<0.001
Aging	0.101022	2	0.050511	249.391	<0.001
Material	0.263723	2	0.131861	651.047	<0.001
Aging × Material	0.141808	4	0.035452	175.039	<0.001
Error	0.012760	63	0.000203		
Total	0.982195	72			

Post-hoc Tukey HSD analysis revealed significant differences in the monoclinic phase fraction among the aging-time groups ($p < 0.05$). The mean monoclinic phase fraction increased from 0.032 ^{a} ± 0.001 in the control group to 0.085 ^{b} ± 0.014 after 5 h and

0.124 [c] ± 0.023 after 10 h of hydrothermal aging. The mean monoclinic phase fraction was 0.032 [a] ± 0.001 for UTML, 0.043 [b] ± 0.003 for STML, and 0.166 [c] ± 0.021 for ML.

Compared with the control group, hydrothermal aging for 5 and 10 h increased the mean monoclinic phase fraction in all material groups, with the greatest increase observed in the ML group (Figures 2–4).

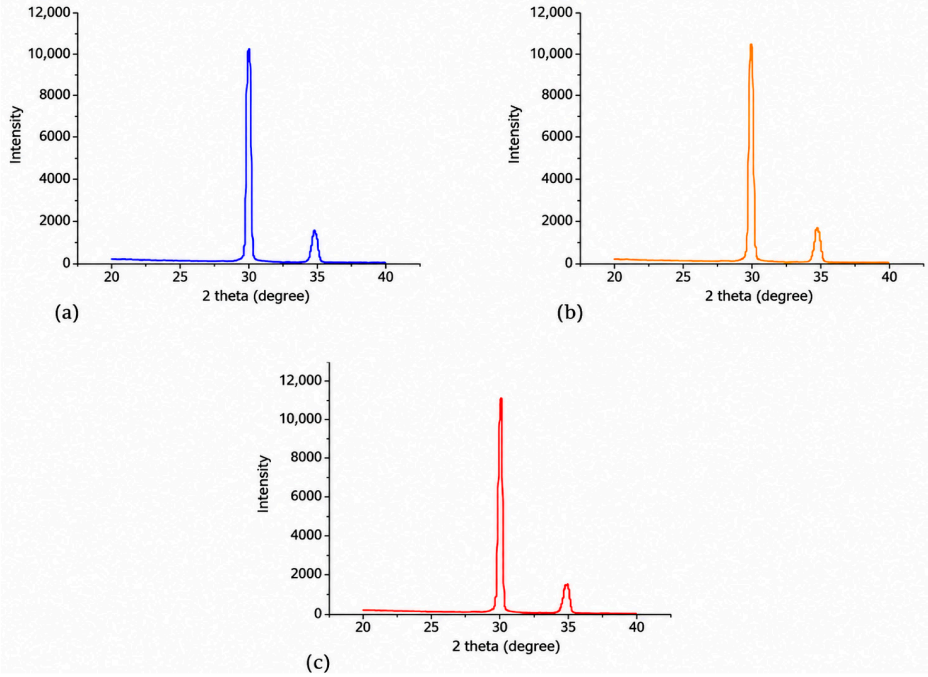


Figure 2. (**a**) XRD graph of the UTML control group; (**b**) XRD graph of the UTML 5-h aging group; (**c**) XRD graph of the UTML 10-h aging group.

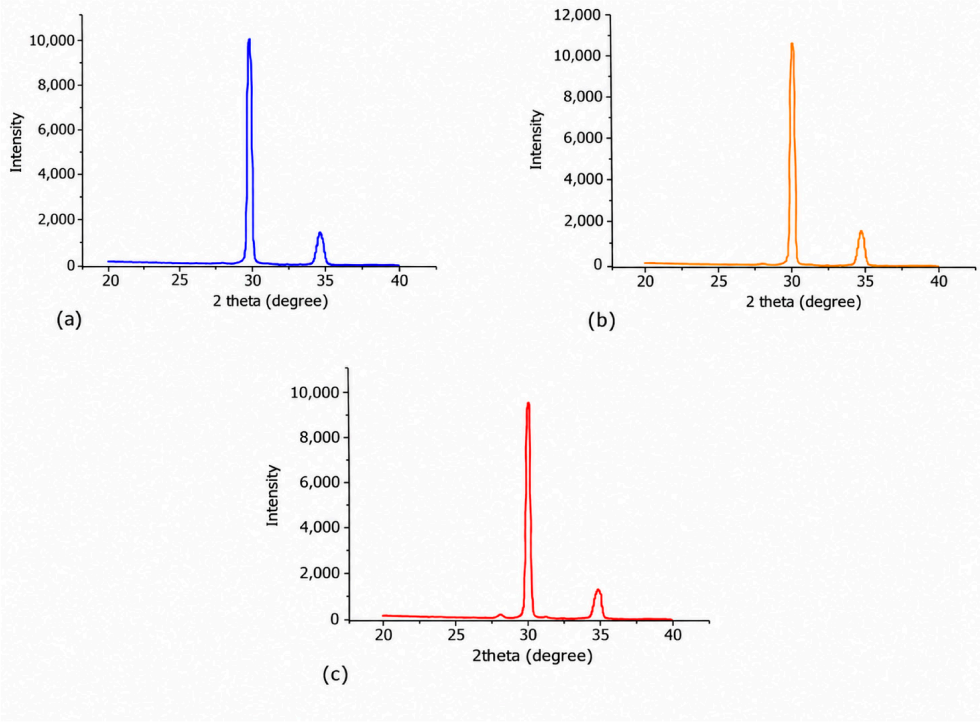


Figure 3. (**a**) XRD graph of the STML control group; (**b**) XRD graph of the STML 5-h aging group; (**c**) XRD graph of the STML 10-h aging group.

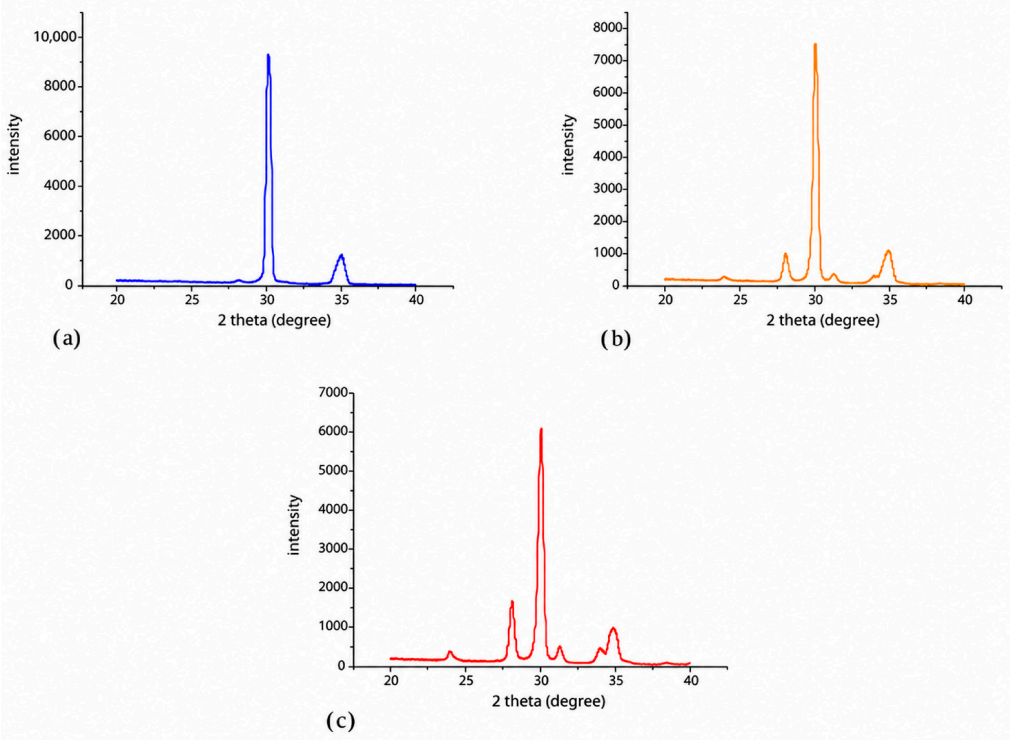


Figure 4. (**a**) XRD graph of the ML control group; (**b**) XRD graph of the ML 5-h aging group; (**c**) XRD graph of the ML 10-h aging group.

3.4. Scanning Electron Microscopy (SEM) Analysis

In the UTML groups, hydrothermally aged specimens exhibited more pronounced surface irregularities, including pits and grooves, whereas the control specimens showed comparatively smoother surfaces. After 5 h of hydrothermal aging, the UTML specimens exhibited a relatively homogeneous surface morphology with shallow depressions and protrusions, whereas after 10 h, the surface appeared more heterogeneous, with more pronounced morphological irregularities (Figure 5).

In the STML groups, the control and 5-h aged specimens exhibited generally comparable surface morphologies, with relatively homogeneous surfaces and only limited localized irregularities, whereas the 10-h aged specimens showed a more heterogeneous surface morphology characterized by more pronounced and localized surface irregularities (Figure 6).

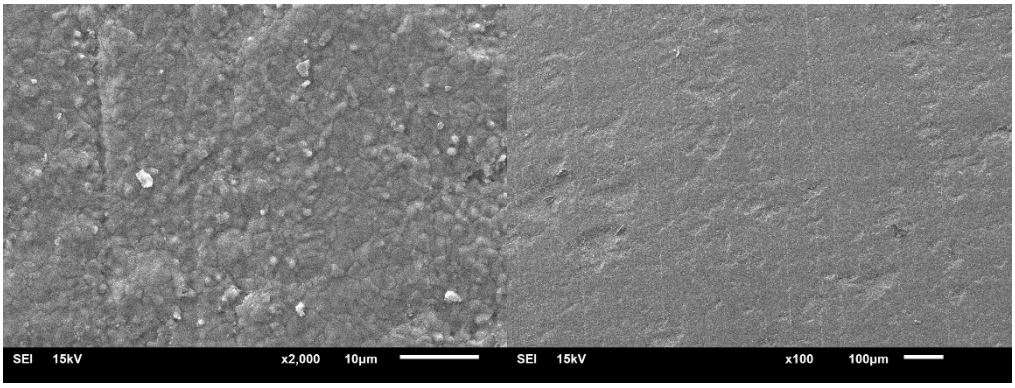


Figure 5. *Cont.*

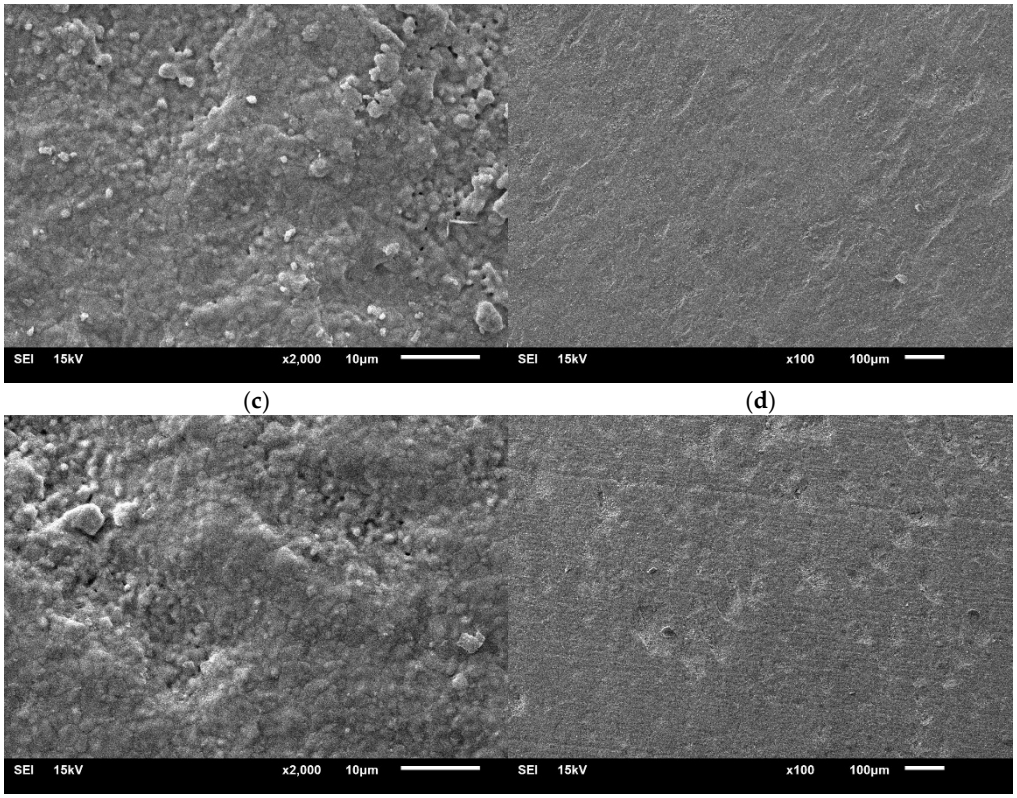


Figure 5. SEM images of the UTML group. (**a**) control, ×2000; (**b**) control, ×100; (**c**) 5-h aging, ×2000; (**d**) 5-h aging, ×100; (**e**) 10-h aging, ×2000; (**f**) 10-h aging, ×100.

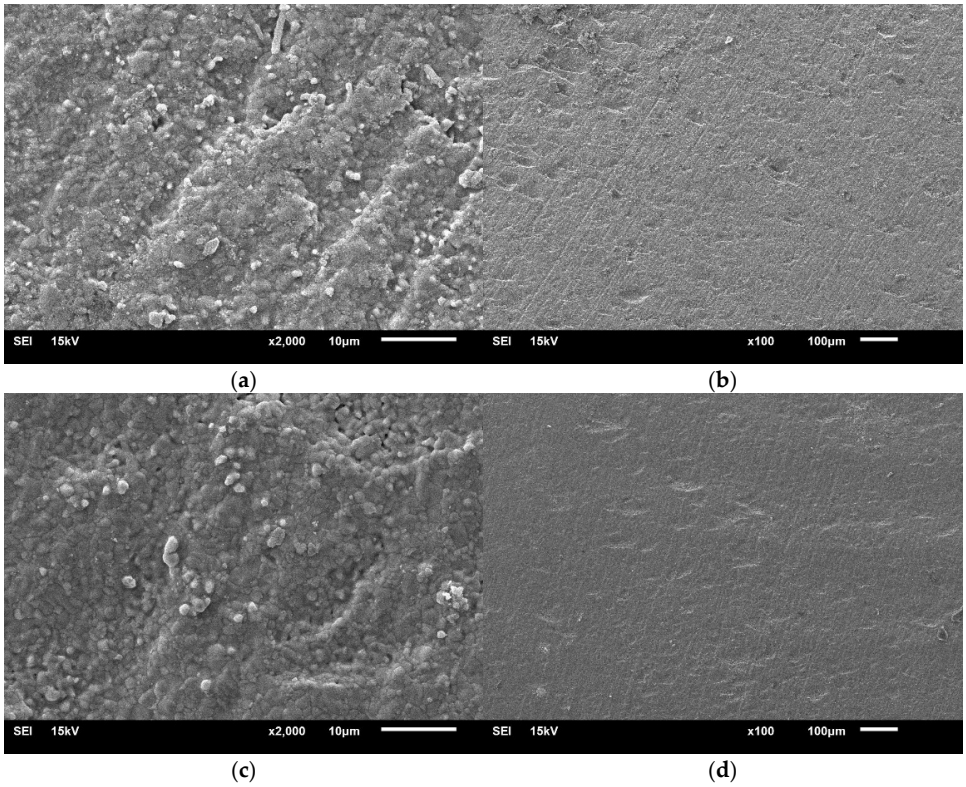
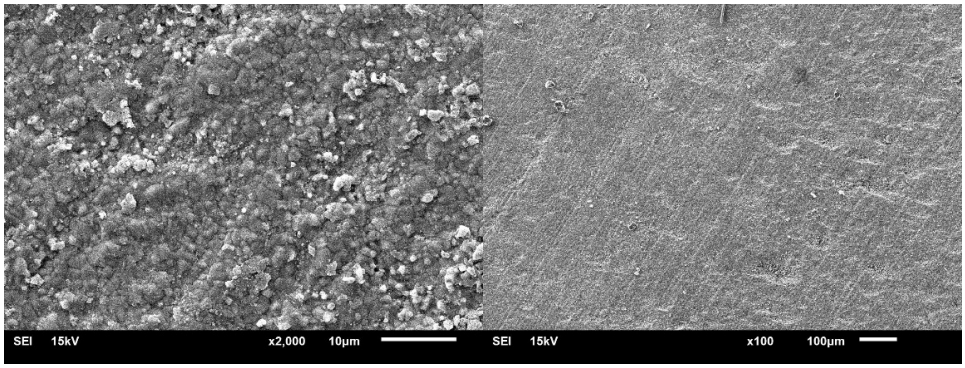


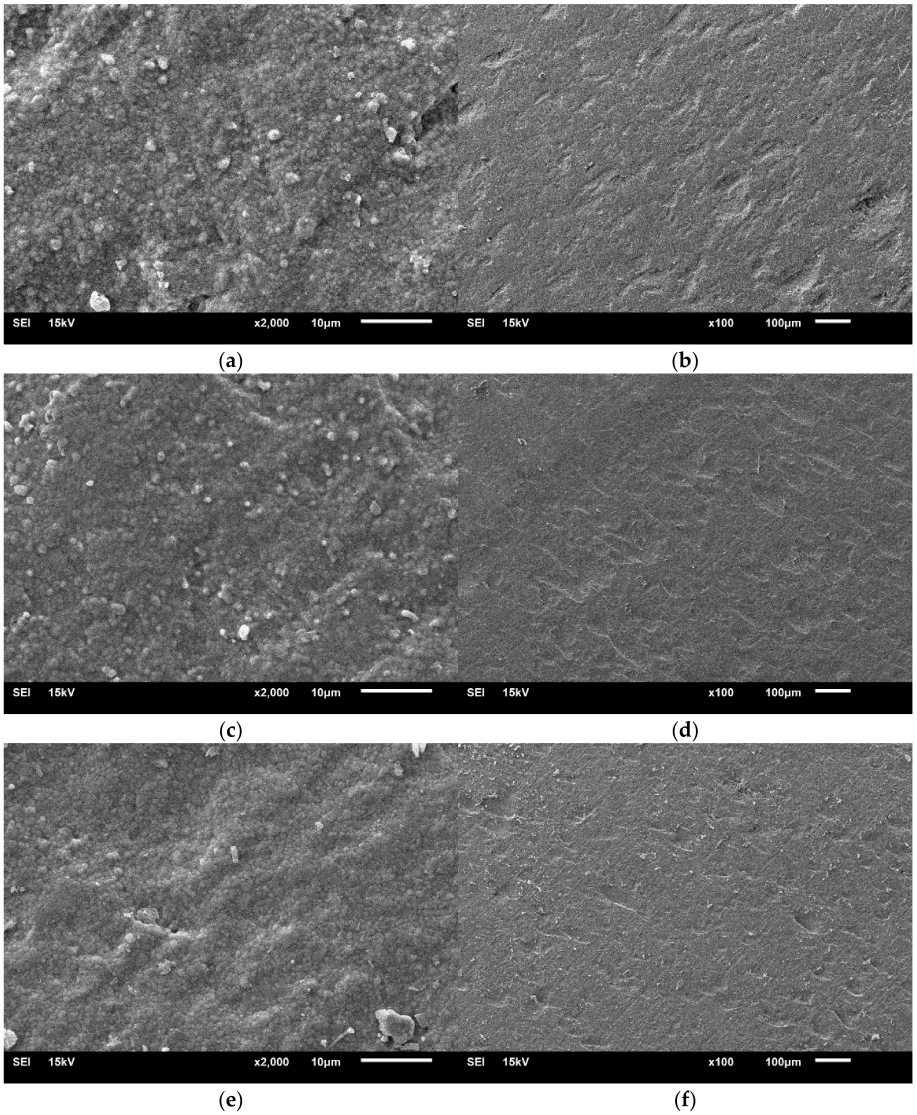
Figure 6. *Cont.*



(e) (f)

Figure 6. SEM images of the STML group. (**a**) control, ×2000; (**b**) control, ×100; (**c**) 5-h aging, ×2000; (**d**) 5-h aging, ×100; (**e**) 10-h aging, ×2000; (**f**) 10-h aging, ×100.

In contrast to the UTML and STML groups, the ML specimens exhibited a different morphological response to hydrothermal aging, with a progressively more homogeneous surface appearance as the aging duration increased (Figure 7).



(a) (b)

(c) (d)

(e) (f)

Figure 7. SEM images of the ML group. (**a**) control, ×2000; (**b**) control, ×100; (**c**) 5-h aging, ×2000; (**d**) 5-h aging, ×100; (**e**) 10-h aging, ×2000; (**f**) 10-h aging, ×100.

3.5. Biaxial Flexural Strength Test

Two-way ANOVA revealed significant effects of both aging time ($p = 0.003$) and material type ($p < 0.001$) on BFS values, as well as a significant interaction between aging time and material type ($p = 0.006$) (Table 4).

Table 4. Two-way Variance Analysis of Biaxial Flexural Strength Values.

Source of Variation	Sum of Squares (SS)	Degrees of Freedom (df)	Mean Square (MS)	F	*p*
Intercept	1,212,763.799	1	1,212,763.799	4.883×10^3	<0.001
Aging	3110.388	2	1555.194	6.262	0.003
Material	62,533.933	2	31,266.966	125.896	<0.001
Aging × Material	3912.055	4	978.014	3.938	0.006
Error	17,881.616	72	248.356		
Total	1,300,201.790	81			

Post-hoc Tukey HSD analysis was performed to evaluate pairwise differences in BFS values among the hydrothermal aging groups. The mean BFS values were 114.63 ^{a} ± 4.98 MPa in the control group, 122.66 ^{ab} ± 7.31 MPa after 5 h of hydrothermal aging, and 129.80 ^{b} ± 6.47 MPa after 10 h of aging. The 10-h aging group exhibited a significantly higher BFS value than the control group ($p < 0.05$), whereas the 5-h aging group did not differ significantly from either the control or 10-h aging group ($p > 0.05$).

Post-hoc Tukey HSD analysis revealed significant differences in BFS values among the material groups ($p < 0.05$). The mean BFS values were 91.84 ^{a} ± 2.58 MPa for UTML, 116.19 ^{b} ± 2.37 MPa for STML, and 159.06 ^{c} ± 3.82 MPa for ML, with significant differences observed among all three material groups ($p < 0.05$).

Among the materials, ML exhibited the highest mean BFS value, whereas UTML exhibited the lowest. Overall, BFS values showed an increasing trend with prolonged hydrothermal aging; however, the magnitude and pattern of this change varied among the materials, with the UTML group showing no increase after 5 h of aging.

4. Discussion

High-translucency monolithic zirconia restorations, particularly those based on zirconia compositions with increased yttria content such as 4Y-PSZ and 5Y-PSZ, have gained increasing clinical relevance because compositional modifications that increase the proportion of optically favorable phases can improve light transmission and esthetic performance compared with conventional 3Y-TZP. However, these compositional changes also modify the phase constitution, microstructure, and transformation capability of zirconia, resulting in a balance between improved translucency and mechanical performance [8].

Despite these advances, direct exposure of monolithic zirconia restorations to the humid oral environment remains clinically relevant because zirconia may undergo low-temperature degradation (LTD), a hydrothermally driven process associated with tetragonal-to-monoclinic (t→ m) phase transformation. The susceptibility and progression of LTD are strongly influenced by material-related factors, particularly stabilizer type and concentration, grain size, residual stresses, and microstructural characteristics; consequently, zirconia materials with different yttria contents may exhibit substantially different responses to hydrothermal aging [12].

Accordingly, the present study investigated the effects of hydrothermal aging on the optical, microstructural, and mechanical properties of multilayer translucent monolithic zirconia materials with different yttria contents. The findings demonstrated that the effects of hydrothermal aging varied according to both the material type and the property evalu-

ated. Hydrothermal aging significantly affected translucency, monoclinic phase fraction, and biaxial flexural strength, whereas no significant effect was observed on Vickers hardness. Material type, however, significantly influenced all evaluated properties, including translucency, monoclinic phase fraction, Vickers hardness, and biaxial flexural strength. Therefore, the null hypothesis that hydrothermal aging would have no significant effect on the evaluated properties was partially rejected.

The esthetic performance of monolithic zirconia restorations is strongly influenced by their optical properties, particularly translucency, which is closely related to the interaction of light with the phase composition and microstructure of zirconia [25]. Translucency refers to the ability of a material to transmit light while allowing a certain degree of light scattering and is therefore an important determinant of the esthetic appearance of dental restorations and their ability to reproduce the optical characteristics of natural teeth [25,26].

The translucency of monolithic zirconia is determined by a complex interaction among compositional, microstructural, and processing-related factors. Compositional characteristics, including yttria content [2,27], phase constitution [16], additives [16,28,29], and impurities [30], can influence the interaction of light with the zirconia microstructure. Microstructural features such as grain size [31], grain boundaries [16,29,31], porosity and structural defects [32], and birefringence [33] can further modify light transmission and scattering [34,35]. In addition, the degree of sintering [36] and sintering conditions [36,37] contribute to the final optical behavior of zirconia. These optical properties may also be modified by hydrothermal aging through aging-induced changes in the phase composition and microstructure [25,38].

Following hydrothermal aging, changes in the translucency parameter (TP) may vary according to aging duration and material-specific characteristics, including chemical composition, phase constitution, grain size, porosity, surface characteristics, and specimen thickness [38]. These factors may influence the extent to which aging-induced phase and microstructural alterations modify light transmission and scattering, which may explain the variability in translucency changes reported among different zirconia materials and aging protocols [38].

In the present study, hydrothermal aging significantly affected the translucency of the tested zirconia materials, with a greater reduction in TP observed after 10 h than after 5 h of aging. The mean TP value decreased from 8.004 to 6.987 in the 5 h group and from 8.155 to 6.311 in the 10 h group. This finding indicates that prolonged hydrothermal exposure may progressively reduce light transmission through multilayer translucent zirconia. Aging-related changes in optical behavior have been reported for multilayer zirconia materials, although the magnitude and direction of these changes appear to depend on material composition, microstructure, and aging conditions [17,38].

In the present study, material type significantly influenced translucency, with UTML exhibiting the highest mean TP value, followed by STML and ML. This material-dependent difference may be primarily related to variations in yttria content and phase constitution, as increasing yttria content alters the relative proportions of tetragonal and cubic phases and reduces birefringence-related light scattering, thereby contributing to improved translucency [19,25]. The higher mean translucency values observed for UTML and STML compared with ML are consistent with the findings of Kolakarnprasert et al. [19], who reported that UTML and STML exhibited greater translucency than ML. However, unlike the present study, in which UTML exhibited significantly higher translucency than STML, Kolakarnprasert et al. [19] found no significant difference in translucency between these two materials. This discrepancy suggests that yttria content and cubic phase fraction alone may not fully determine the optical behavior of multilayer zirconia, and that differences

in grain size, pigment composition, specimen thickness, and experimental conditions may also contribute to the observed translucency [19,25].

The aging-related decrease in translucency observed in the present study may also be associated with the concurrent changes in phase composition. XRD analysis demonstrated a progressive increase in the monoclinic phase fraction with hydrothermal aging, suggesting that the aging-induced tetragonal-to-monoclinic (t→ m) transformation may have contributed to the observed reduction in TP. The formation of the monoclinic phase, together with aging-induced microstructural alterations, may increase optical heterogeneity and light scattering within the material, thereby reducing light transmission [38,39].

Specimen thickness is another important factor that may influence both baseline translucency and the magnitude of translucency changes induced by hydrothermal aging. Abdelbary et al. [40] reported that 0.5-mm-thick zirconia specimens exhibited a significant reduction in TP after 5 h of hydrothermal aging, whereas thicker specimens ranging from 0.8 to 1.2 mm were not significantly affected. This finding is consistent with evidence indicating that thinner zirconia specimens may exhibit greater aging-related changes in translucency [38]. In contrast, the present study demonstrated a significant reduction in TP in 1.2-mm-thick specimens, suggesting that aging-related translucency changes may also depend on material-specific characteristics and experimental conditions. Walczak et al. [41] similarly reported a reduction in translucency after 5 h of autoclave aging, although the magnitude of the change varied among the zirconia materials tested. Putra et al. [4] further demonstrated that, in 1-mm-thick specimens, the direction and magnitude of aging-related changes in total transmittance varied among zirconia materials. Collectively, these findings indicate that the optical response of zirconia to hydrothermal aging cannot be attributed to aging duration alone but is influenced by the interaction among specimen thickness, material composition, and microstructural characteristics [4,39–41].

The effect of hydrothermal aging on zirconia translucency also appears to be time-dependent, although the relationship is not necessarily linear. A systematic review and meta-analysis reported that aging duration contributed to variations in the optical response of monolithic translucent Y-TZP; however, the pooled results suggested that translucency was generally stable following hydrothermal aging at 134 °C and 0.2 MPa for periods of up to 20 h [42]. This finding differs partly from the present results, in which a greater reduction in TP was observed in the 10 h aging group than in the 5 h group, suggesting that even relatively short aging periods may produce detectable optical changes depending on the composition and microstructure of the zirconia material. Nevertheless, although the reduction in TP observed in the present study was statistically significant, its clinical relevance should be interpreted with reference to established perceptibility and acceptability thresholds for changes in translucency [38,42].

Variations in the chemical composition of zirconia, particularly in Y_2O_3, Al_2O_3, and other oxide contents, may contribute not only to differences in translucency but also to variations in susceptibility to hydrothermal degradation [38,43,44]. In addition to the stabilizing effect of Y_2O_3 on phase constitution, minor oxide additives may modify grain-boundary chemistry and thereby influence the progression of LTD. Zhang et al. [43] and Nogiwa-Valdez et al. [44] demonstrated that small amounts of Al_2O_3 and La_2O_3 can improve the resistance of zirconia to hydrothermal degradation. In particular, Nogiwa-Valdez et al. [44] reported that La_2O_3 and Al_2O_3 co-doping markedly reduced the hydrothermal degradation kinetics of 3Y-TZP without substantially compromising its mechanical properties. Therefore, differences in the aging behavior of zirconia materials cannot be attributed solely to yttria content, because minor oxide additives and their effects on grain-boundary chemistry may also influence both optical properties and LTD resistance [39,44,45]. Sintering conditions represent an additional factor influencing translucency, as the degree of densification, resid-

ual porosity, and grain size determine the extent of light scattering within the zirconia microstructure [37,46,47]. In particular, Stawarczyk et al. [46] demonstrated that sintering parameters and grain size are significantly associated with the optical properties of zirconia ceramics. The type and concentration of dopant cations may also influence grain-boundary characteristics and the hydrothermal degradation behavior of zirconia [43,44]. Other oxide additives, including SiO_2, Sc_2O_3, Nd_2O_3, MgO, and GeO_2, have also been investigated for modifying the optical and microstructural properties of zirconia [29,47,48]; however, their long-term hydrothermal behavior requires further investigation.

TP and contrast ratio (CR) are commonly used to characterize the translucency of dental materials, and an inverse relationship between these parameters has been reported [26,49]. In the present study, TP was used to quantify translucency because it provides a direct numerical representation of the color difference in a material measured over black and white backgrounds [26].

Hydrothermal aging in a steam autoclave is widely used as an accelerated method to investigate the susceptibility of zirconia to LTD under controlled conditions. Chevalier [10] proposed that 1 h of autoclave aging at 134 °C may theoretically correspond to approximately 3–4 years of in-vivo aging. Based on this theoretical estimation, the 5- and 10-h aging periods used in the present study may correspond to approximately 15–20 and 30–40 years of in vivo aging, respectively. However, these equivalences should be interpreted cautiously because autoclave aging accelerates hydrothermal degradation under standardized conditions and does not reproduce the complex combination of thermal, chemical, pH-related, and mechanical challenges present in the oral environment [10,12].

Because Y-TZP has a metastable structure, its susceptibility to the tetragonal-to-monoclinic (t→ m) phase transformation associated with LTD is strongly influenced by material- and processing-related factors, including yttria content, phase constitution, grain size, microstructural characteristics, residual stresses, manufacturing procedures, and aging conditions [50–52]. During hydrothermal exposure, water species can interact with oxygen-vacancy-related defects and grain-boundary regions, facilitating destabilization of the tetragonal phase and promoting the nucleation and propagation of the monoclinic transformation from the exposed surface toward the bulk of the material [12]. Because LTD may alter the phase stability and long-term behavior of zirconia restorations, its progression under hydrothermal conditions has been extensively investigated [10,12,53]. In the present study, XRD analysis demonstrated a progressive increase in the monoclinic phase fraction with increasing hydrothermal aging duration, from 0.032 in the control condition to 0.085 after 5 h and 0.124 after 10 h of aging. These findings provide direct evidence that the phase constitution of the tested zirconia materials was progressively altered by hydrothermal exposure, although the extent of transformation was material-dependent. Putra et al. [4] reported an increase in the monoclinic phase fraction of STML following 50 h of hydrothermal aging at 134 °C, whereas UTML remained resistant to LTD, with no detectable monoclinic phase transformation even after 100 h of aging. In contrast, the present study demonstrated an overall aging-related increase in the monoclinic phase fraction within the substantially shorter 5- and 10-h aging periods, although the extent of transformation was material-dependent. The discrepancy between the two studies may be related to differences in specimen preparation, surface condition, analytical procedures, and other experimental parameters, in addition to material-specific microstructural characteristics. Therefore, aging duration alone may not fully explain the susceptibility of multilayer zirconia to LTD, and comparisons among studies should also consider differences in experimental methodology and material characteristics [4]. Flinn et al. [54] demonstrated that the progression of the t→ m transformation during hydrothermal aging was strongly material-dependent. Among the zirconia materials evaluated, ZirTough exhibited a slower increase in monoclinic phase frac-

tion and a smaller reduction in flexural strength than the other materials, indicating greater resistance to hydrothermal degradation [54]. Importantly, their findings also showed that prolonged aging and extensive monoclinic transformation were ultimately associated with deterioration of flexural strength, suggesting that the mechanical consequences of LTD may depend on both the extent and progression of phase transformation. In contrast to the prolonged hydrothermal aging periods of up to 200 h investigated by Flinn et al. [54], the present study evaluated relatively early stages of hydrothermal aging at 5 and 10 h under the same temperature and pressure conditions (134 °C and 0.2 MPa). Although the monoclinic phase fraction progressively increased with aging in the present study, biaxial flexural strength did not decrease and instead showed an overall increasing trend. These findings suggest that the early stages of hydrothermal aging may not adversely affect mechanical strength, whereas prolonged aging and more extensive degradation may eventually lead to deterioration of mechanical properties.

While Flinn et al. [55] reported that the flexural strength of ML zirconia was not significantly affected by aging duration, the present study demonstrated a more pronounced aging-related variation in biaxial flexural strength in the ML group than in the UTML and STML groups. This difference further supports the material-dependent nature of the mechanical response to hydrothermal aging and suggests that zirconia compositions with different phase constitutions may respond differently even when subjected to comparable hydrothermal conditions. Increasing yttria content modifies the phase constitution and microstructure of zirconia by altering the relative proportions of tetragonal and cubic phases, thereby generally improving translucency while reducing flexural strength and transformation-toughening potential [8,56]. This compositional trade-off is particularly relevant to the interpretation of hydrothermal aging, because zirconia materials with different yttria contents and phase constitutions may exhibit different susceptibilities to t→ m transformation and, consequently, different mechanical responses during LTD [8,56]. The higher translucency associated with an increased cubic phase fraction can be explained by the optical isotropy of c-ZrO_2, in which the refractive index is independent of crystallographic orientation, thereby reducing birefringence-related light scattering at grain boundaries. In contrast, t-ZrO_2 is optically anisotropic, and differences in crystallographic orientation between adjacent tetragonal grains produce refractive-index discontinuities at grain boundaries, increasing light scattering and reducing light transmission [25,45]. Grain size may further influence the optical behavior of zirconia by modifying the number and characteristics of grain boundaries through which light propagates. Although larger grains may reduce the number of grain boundaries and thereby decrease grain-boundary-related light scattering, the relationship between grain size and translucency is not linear and may also depend on phase constitution, porosity, refractive-index differences, and the relationship between grain size and the wavelength of incident light [25,45]. Therefore, grain size alone cannot account for the differences in translucency observed among contemporary multilayer zirconia materials [25]. In addition to yttria content, sintering conditions, particularly the final sintering temperature, may influence the phase constitution and microstructure of zirconia by modifying grain growth, densification, porosity, and cubic phase content [25,56]. Higher sintering temperatures may promote grain growth and reduce residual porosity, which can decrease light scattering and improve translucency; however, this relationship is material-dependent, and excessive temperatures may adversely affect the microstructure and optical behavior of zirconia [25]. In the present study, the specimens were sintered according to the manufacturer-recommended protocols, with ML sintered at 1500 °C and UTML and STML at 1550 °C [19]. These material-specific sintering temperatures are consistent with the different compositions and microstructures of the three zirconia grades and should therefore be considered together with yttria content and phase constitution when

interpreting the observed differences in optical and mechanical properties [19,25]. Residual porosity and impurities represent additional microstructural factors that may influence the translucency of zirconia [30]. Pores and impurity-containing regions introduce refractive-index discontinuities within the zirconia microstructure, thereby increasing light scattering and reducing light transmission [25,46]. The optical effect of porosity may be particularly relevant when pore dimensions approach the wavelength range of visible light, indicating that not only the amount but also the size and distribution of pores may contribute to the final translucency of zirconia [25].

Changes in translucency following hydrothermal aging have frequently been associated with aging-induced t→ m phase transformation; however, monoclinic phase content alone may not fully explain the optical changes observed in zirconia. Putra et al. [4] reported that an increase in monoclinic phase content could be accompanied by increased light transmission in some zirconia materials, whereas Fathy et al. [57] reported a reduction in TP after 15 h of hydrothermal aging, accompanied by an increase in monoclinic phase content. The reduction in translucency observed by Fathy et al. [57] may be associated with aging-related phase transformation and accompanying microstructural alterations that increase light scattering. Similarly, the present study demonstrated a reduction in TP accompanied by an overall increase in monoclinic phase content following hydrothermal aging, consistent with the findings reported by Fathy et al. [57]. These contrasting findings suggest that the effect of t→ m transformation on translucency is influenced by additional material- and microstructure-related factors, including phase distribution, grain characteristics, porosity, and chemical composition [4,38,57]. Therefore, the optical consequences of hydrothermal aging should be interpreted as the combined result of phase and microstructural changes rather than changes in monoclinic phase fraction alone [4,38,57]. The aging-related increase in translucency reported by Putra et al. [4] and Kim et al. [58] may be associated in part with compositional and microstructural changes involving metal oxide pigments and the cubic phase. Certain metal oxide additives may influence phase stability and favor the presence of optically isotropic cubic zirconia, which could reduce birefringence-related light scattering and thereby contribute to increased light transmission during hydrothermal aging [4,58]. However, this mechanism should be interpreted cautiously because changes in translucency during aging are likely determined by the combined effects of phase constitution, pigment composition, grain characteristics, and other microstructural alterations rather than by cubic phase content alone [4,25,58]. Similarly, Choi et al. [59] proposed that the aging-related increase in translucency could be associated with changes in the cubic phase, whose optical isotropy may reduce birefringence-related light scattering. However, because their XRD analysis primarily evaluated the aging-induced increase in monoclinic phase content rather than directly quantifying changes in the cubic phase fraction, this mechanism remains a possible explanation rather than a directly demonstrated consequence of hydrothermal aging [59]. Another potential mechanism involves the segregation of trivalent dopant ions at grain boundaries, which may modify grain-boundary chemistry and phase stability and thereby influence the susceptibility of zirconia to hydrothermal degradation [38]. Such compositional changes at grain boundaries may indirectly affect translucency by altering the extent and distribution of aging-induced phase transformation and the associated microstructural changes. In addition, differences in grain size and in the spatial distribution of tetragonal and monoclinic phases may modify the number and characteristics of optical interfaces within the microstructure, thereby influencing light scattering and transmission [38].

Several compositional and microstructural strategies have been investigated to improve zirconia translucency, including a reduction in light-scattering additives and impurities, control of grain size, and an increase in the proportion of the optically isotropic cubic

phase [25,30,46]. However, modifications intended to enhance translucency may simultaneously influence the mechanical properties and hydrothermal stability of zirconia. In particular, reducing the Al_2O_3 content can improve translucency by decreasing light scattering from alumina particles, but excessively low Al_2O_3 concentrations may reduce resistance to hydrothermal degradation [30,43]. Similarly, increasing the cubic phase fraction can improve light transmission but may reduce transformation-toughening capability and consequently compromise strength and fracture toughness [8]. Therefore, the development of highly translucent zirconia requires a balance among optical performance, mechanical reliability, and resistance to hydrothermal degradation rather than optimization of translucency alone. The improved translucency of cubic-rich zirconia is accompanied by lower mechanical performance compared with predominantly tetragonal zirconia [8,60]. This reduction is primarily related to the limited transformation-toughening capability of the stable cubic phase, resulting in generally lower flexural strength and fracture toughness as the cubic phase fraction increases [8,60]. Zhang [45] proposed that reducing the grain size of tetragonal Y-TZP to the nanometer scale may improve translucency by decreasing birefringence-related light scattering. However, grain size must be carefully controlled because it also influences tetragonal phase stability and transformation-toughening behavior; therefore, optimization of grain size requires a balance between optical and mechanical properties [45,61].

The effect of hydrothermal aging on the flexural strength of zirconia is influenced by both material-related and experimental factors, including composition, microstructure, sintering conditions, surface treatment, aging duration, and aging temperature [13,16,62–64]. Consequently, hydrothermal aging may increase, decrease, or have no significant effect on flexural strength depending on the extent of phase transformation and the specific characteristics of the zirconia material [13,62–64]. In the present study, hydrothermal aging significantly influenced the biaxial flexural strength of the tested monolithic zirconia materials, with an overall tendency toward increased strength after 5 and 10 h of aging. However, the magnitude and pattern of this response differed among the materials, indicating that the mechanical effect of hydrothermal aging was material-dependent. Previous studies have similarly demonstrated that the effect of hydrothermal aging on flexural strength is strongly dependent on zirconia composition and microstructure [13,62,65]. Pereira et al. [13] and Amat et al. [65] showed that zirconia materials with different microstructural characteristics may exhibit different mechanical responses following hydrothermal exposure, whereas Camposilvan et al. [62] further associated the response to prolonged hydrothermal aging with differences in zirconia composition. Consistent with the present findings, zirconia compositions with lower yttria content have generally exhibited higher flexural strength after hydrothermal aging, reflecting the greater contribution of the metastable tetragonal phase and its transformation-toughening capability [62]. However, the present study additionally evaluated the relationship between aging-induced monoclinic phase transformation and biaxial flexural strength across zirconia materials with different yttria contents. Despite the progressive increase in monoclinic phase fraction with aging, biaxial flexural strength did not decrease and instead showed an overall increasing trend. This finding suggests that aging-induced t→ m transformation does not necessarily cause an immediate reduction in mechanical strength and that its mechanical effect may depend on the extent of transformation. The three zirconia materials investigated in the present study represent distinct yttria-stabilized compositions, with ML, STML, and UTML corresponding approximately to 3Y-, 4Y-, and 5Y-PSZ, respectively [19]. These compositional differences are accompanied by substantial variations in cubic phase fraction and grain size, which may contribute to their different mechanical responses to hydrothermal aging [19].

Borchers et al. [66] reported that hydrothermal aging increased the monoclinic phase content of 3Y-TZP without significantly affecting biaxial flexural strength, indicating that the occurrence of t→ m transformation does not necessarily result in an immediate deterioration of bulk mechanical strength. Similarly, Alghazzawi et al. [67] observed an increase in monoclinic phase content following aging without a statistically significant reduction in biaxial flexural strength. These findings have been attributed to the initially superficial nature of the aging-induced phase transformation, which may limit its influence on the bulk mechanical behavior of zirconia [66,67]. However, when the aging-induced t→ m transformation progresses beyond the superficial layer and extends deeper into the material, the accumulation of transformation-related defects may ultimately compromise flexural strength [16]. Conversely, a limited degree of t→ m transformation may initially contribute to increased flexural strength through transformation-induced compressive stresses that oppose crack propagation [68,69].

Flinn et al. [55] demonstrated that the mechanical response to prolonged hydrothermal aging was material-dependent, with flexural strength decreasing in some translucent zirconia materials while remaining relatively stable in others. Inokoshi et al. [70] similarly demonstrated material-dependent LTD behavior and further showed that surface treatment can substantially modify hydrothermal aging resistance in different zirconia systems. Pereira et al. [13] demonstrated that zirconia susceptibility to LTD is strongly influenced by yttria content and the resulting phase constitution. In their study, the predominantly tetragonal ML zirconia exhibited aging-induced monoclinic transformation, whereas the more highly stabilized STML and UTML materials, characterized by different phase constitutions associated with their higher yttria contents, showed substantially greater resistance to hydrothermal degradation [13]. This behavior can be explained by the increased phase stability associated with higher stabilizer concentrations, which reduces the susceptibility of tetragonal grains to aging-induced t→ m transformation [13,71]. However, this improved hydrothermal stability is accompanied by a reduction in transformation-toughening capability and therefore does not necessarily correspond to superior mechanical strength.

The present study focused primarily on aging-induced changes in the monoclinic phase fraction; therefore, the complete phase constitution, particularly the relative fractions of tetragonal and cubic phases, was not quantitatively characterized. Future studies incorporating quantitative characterization of the complete phase constitution may provide further insight into the relationships among phase composition, translucency, hydrothermal stability, and mechanical behavior. Furthermore, although XRD analysis enabled evaluation of aging-induced changes in the monoclinic phase fraction, the depth of the transformed layer was not quantitatively assessed. Because hydrothermal degradation may progressively extend from the surface into the material, future studies should consider the depth of phase transformation when evaluating the long-term effects of hydrothermal aging [52]. In addition, the present investigation was conducted under controlled in vitro conditions using standardized disc-shaped specimens and hydrothermal aging in an autoclave. Although this approach enables controlled evaluation of LTD, it does not fully reproduce the complex oral environment, in which zirconia restorations are simultaneously exposed to thermal fluctuations, moisture, pH changes, and cyclic mechanical loading. Therefore, future studies should combine hydrothermal aging with thermocycling and mechanical fatigue and incorporate quantitative phase analysis to provide a more comprehensive understanding of the long-term optical, structural, and mechanical behavior of multilayer zirconia.

The observed differences in hydrothermal aging behavior among zirconia materials highlight the importance of material composition and resistance to hydrothermal phase transformation in the development of zirconia-based dental ceramics. However, because the present study evaluated zirconia materials intended for prosthetic restorations, di-

rect recommendations for dental implant manufacturing cannot be made without further investigations using implant-specific materials and testing conditions.

Although biaxial flexural strength was evaluated under standardized loading conditions in accordance with ISO 6872, this test does not fully reproduce the nonuniform, multidirectional, and cyclic mechanical loading conditions experienced by dental prostheses during clinical function.

Furthermore, the phase transformation was evaluated using XRD, which primarily provides information from the near-surface region of zirconia specimens. Therefore, the reported monoclinic phase fractions should not be interpreted as representative of the entire specimen volume.

5. Conclusions

Hydrothermal aging induced material-dependent tetragonal-to-monoclinic (t→ m) phase transformation, with UTML showing the greatest resistance to monoclinic transformation and ML exhibiting the highest monoclinic phase fraction after aging. Translucency differed significantly among the tested zirconia materials, with UTML exhibiting the highest TP values, followed by STML and ML, while prolonged hydrothermal aging resulted in lower TP values. Hydrothermal aging promoted t→ m phase transformation without reducing biaxial flexural strength; instead, an overall tendency toward increased biaxial flexural strength was observed, although the magnitude of this response was material-dependent. Vickers hardness was not significantly affected by hydrothermal aging; however, material type had a significant effect, with UTML exhibiting significantly higher hardness than ML. These findings demonstrate that the optical, phase, and mechanical responses of multilayer zirconia to hydrothermal aging are strongly material-dependent and should be interpreted in relation to differences in composition and phase constitution. Further studies are warranted to clarify the long-term clinical implications of these material-dependent responses.

Author Contributions: M.A. designed the study and acquired and analyzed the data. M.A.U. drafted and edited the manuscript, supervised the study, and conducted the experimental design. M.A. reviewed and revised the first draft. All authors have read and agreed to the published version of the manuscript.

Funding: The required materials and laboratory expenses were supported by the Scientific Research Projects Unit (BAP) of Recep Tayyip Erdoğan University under project code TDH-2021-1246. This study was also supported by the Recep Tayyip Erdoğan University Development Foundation (Grant number: 020260080170583).

Institutional Review Board Statement: Not applicable.

Informed Consent Statement: Not applicable.

Data Availability Statement: The datasets generated and/or analyzed during the current study are available from the corresponding author upon reasonable request.

Acknowledgments: This study was conducted at the Department of Prosthodontics, Atatürk University, in collaboration with the Research and Central Laboratories of the Faculty of Dentistry, Recep Tayyip Erdoğan University.

Conflicts of Interest: The authors declare no conflicts of interest.

Abbreviations

UTML	Ultra Translucent Multi-Layered
STML	Super Translucent Multi-Layered
ML	Multi-Layered

XRD	X-ray diffractometer
SEM	Scanning electron microscope
LTD	Low-temperature degradation
t→ m	tetragonal-to-monoclinic
TP	Translucency Parameter
BFS	Biaxial Flexural Strength
N	Newton
HV	Vickers Surface Hardness Values
CAD-CAM	Computer-Aided Design-Computer-Aided Manufacturing

References

1. Denry, I.; Kelly, J.R. State of the art of zirconia for dental applications. *Dent. Mater.* **2008**, *24*, 299–307. [CrossRef] [PubMed]
2. Denry, I.; Kelly, J.R. Emerging ceramic-based materials for dentistry. *J. Dent. Res.* **2014**, *93*, 1235–1242. [CrossRef]
3. Koutayas, S.O.; Vagkopoulou, T.; Pelekanos, S.; Koidis, P.; Strub, J.R. Zirconia in dentistry: Part 2. Evidence-based clinical breakthrough. *Eur. J. Esthet. Dent.* **2009**, *4*, 348–380.
4. Putra, A.; Chung, K.H.; Flinn, B.D.; Kuykendall, T.; Zheng, C.; Harada, K.; Raigrodski, A.J. Effect of hydrothermal treatment on light transmission of translucent zirconias. *J. Prosthet. Dent.* **2017**, *118*, 422–429. [CrossRef] [PubMed]
5. Cattani-Lorente, M.; Durual, S.; Amez-Droz, M.; Wiskott, H.W.; Scherrer, S.S. Hydrothermal degradation of a 3Y-TZP translucent dental ceramic: A comparison of numerical predictions with experimental data after 2 years of aging. *Dent. Mater.* **2016**, *32*, 394–402. [CrossRef] [PubMed]
6. Nakamura, K.; Harada, A.; Ono, M.; Shibasaki, H.; Kanno, T.; Niwano, Y.; Adolfsson, E.; Milleding, P.; Örtengren, U. Effect of low-temperature degradation on the mechanical and microstructural properties of tooth-colored 3Y-TZP ceramics. *J. Mech. Behav. Biomed. Mater.* **2016**, *53*, 301–311. [CrossRef]
7. Manziuc, M.; Gasparik, C.; Negucioiu, M.; Constantiniuc, M.; Burde, A.; Vlas, I.; Dudea, D. Optical properties of translucent zirconia: A review of the literature. *Eurobiotech J.* **2019**, *3*, 45–51. [CrossRef]
8. Cesar, P.F.; Miranda, R.B.P.; Santos, K.F.; Scherrer, S.S.; Zhang, Y. Recent advances in dental zirconia: 15 years of material and processing evolution. *Dent. Mater.* **2024**, *40*, 824–836. [CrossRef] [PubMed]
9. Djaker, N.; Wulfman, C.; Sadoun, M.; Lamy de la Chapelle, M. Zirconia dental implants degradation by confocal Raman microspectroscopy: Analytical simulation and experiments. *Biomed. Opt. Express* **2013**, *4*, 725–731. [CrossRef] [PubMed]
10. Chevalier, J. What future for zirconia as a biomaterial? *Biomaterials* **2006**, *27*, 535–543. [CrossRef] [PubMed]
11. Pandoleon, P.; Kontonasaki, E.; Kantiranis, N.; Pliatsikas, N.; Patsalas, P.; Papadopoulou, L.; Zorba, T.; Paraskevopoulos, K.M.; Koidis, P. Aging of 3Y-TZP dental zirconia and yttrium depletion. *Dent. Mater.* **2017**, *33*, e385–e392. [CrossRef] [PubMed]
12. Lughi, V.; Sergo, V. Low temperature degradation -aging- of zirconia: A critical review of the relevant aspects in dentistry. *Dent. Mater.* **2010**, *26*, 807–820. [CrossRef] [PubMed]
13. Pereira, G.K.R.; Guilardi, L.F.; Dapieve, K.S.; Kleverlaan, C.J.; Rippe, M.P.; Valandro, L.F. Mechanical reliability, fatigue strength and survival analysis of new polycrystalline translucent zirconia ceramics for monolithic restorations. *J. Mech. Behav. Biomed. Mater.* **2018**, *85*, 57–65. [CrossRef] [PubMed]
14. De Souza, G.M.; Zykus, A.; Ghahnavyeh, R.R.; Lawrence, S.K.; Bahr, D.F. Effect of accelerated aging on dental zirconia-based materials. *J. Mech. Behav. Biomed. Mater.* **2017**, *65*, 256–263. [CrossRef] [PubMed]
15. Stawarczyk, B.; Keul, C.; Eichberger, M.; Figge, D.; Edelhoff, D.; Lümkemanne, N. Three generations of zirconia: From veneered to monolithic. Part I. *Quintessence Int.* **2017**, *48*, 369–380. [CrossRef] [PubMed]
16. Zhang, F.; Inokoshi, M.; Batuk, M.; Hadermann, J.; Naert, I.; Van Meerbeek, B.; Vleugels, J. Strength, toughness and aging stability of highly-translucent Y-TZP ceramics for dental restorations. *Dent. Mater.* **2016**, *32*, e327–e337. [CrossRef] [PubMed]
17. Ha, S.R.; Choi, Y.S. Effect of hydrothermal aging on dental multilayered zirconia for monolithic restorations: An in vitro study. *Ceram. Int.* **2021**, *47*, 17057–17068. [CrossRef]
18. Saini, R.S.; Madhav, V.N.V.; Kaushik, A.; Gurumurthy, V.; Kanji, M.A.; Alarcón-Sánchez, M.A.; Heboyan, A. Effect of Artificial Ageing on Optical Properties and Mechanical Strength of High-Translucency Zirconia: A Systematic Review and Meta-Analysis. *Int. Dent. J.* **2025**, *75*, 103899. [CrossRef] [PubMed]
19. Kolakarnprasert, N.; Kaizer, M.R.; Kim, D.K.; Zhang, Y. New multi-layered zirconias: Composition, microstructure and translucency. *Dent. Mater.* **2019**, *35*, 797–806. [CrossRef] [PubMed]
20. *ISO I. 6872*; Dentistry-Ceramic Materials. International Organization for Standardization: Geneva, Switzerland, 2008.
21. Johnston, W.M.; Ma, T.; Kienle, B.H. Translucency parameter of colorants for maxillofacial prostheses. *Int. J. Prosthodont.* **1995**, *8*, 79–86. [PubMed]
22. *ISO I. 13356*; Implants for Surgery—Ceramic Materials Based on Yttria-Stabilized Tetragonal Zirconia (Y-TZP). International Standards Organization: Geneva, Switzerland, 2008.

23. Garvie, R.C.; Nicholson, P.S. Phase analysis in zirconia systems. *J. Am. Ceram. Soc.* **1972**, *55*, 303–305. [CrossRef]
24. Ebeid, K.; Wille, S.; Hamdy, A.; Salah, T.; El-Etreby, A.; Kern, M. Effect of changes in sintering parameters on monolithic translucent zirconia. *Dent. Mater.* **2014**, *30*, e419–e424. [CrossRef] [PubMed]
25. Yousry, M.; Hammad, I.; El Halawani, M.; Aboushelib, M. Translucency of recent zirconia materials and material-related variables affecting their translucency: A systematic review and meta-analysis. *BMC Oral Health* **2024**, *24*, 309. [CrossRef] [PubMed]
26. Johnston, W.M. Review of translucency determinations and applications to dental materials. *J. Esthet. Restor. Dent.* **2014**, *26*, 217–223. [CrossRef] [PubMed]
27. Harada, K.; Raigrodski, A.J.; Chung, K.H.; Flinn, B.D.; Dogan, S.; Mancl, L.A. A comparative evaluation of the translucency of zirconias and lithium disilicate for monolithic restorations. *J. Prosthet. Dent.* **2016**, *116*, 257–263. [CrossRef] [PubMed]
28. Samodurova, A.; Kocjan, A.; Swain, M.V.; Kosmač, T. The combined effect of alumina and silica co-doping on the ageing resistance of 3Y-TZP bioceramics. *Acta Biomater.* **2015**, *11*, 477–487. [CrossRef] [PubMed]
29. Nakamura, T.; Nakano, Y.; Usami, H.; Wakabayashi, K.; Ohnishi, H.; Sekino, T.; Yatani, H. Translucency and low-temperature degradation of silica-doped zirconia: A pilot study. *Dent. Mater. J.* **2016**, *35*, 571–577. [CrossRef] [PubMed]
30. Ghodsi, S.; Jafarian, Z. A Review on Translucent Zirconia. *Eur. J. Prosthodont. Restor. Dent.* **2018**, *26*, 62–74. [CrossRef] [PubMed]
31. Stawarczyk, B.; Frevert, K.; Ender, A.; Roos, M.; Sener, B.; Wimmer, T. Comparison of four monolithic zirconia materials with conventional ones: Contrast ratio, grain size, four-point flexural strength and two-body wear. *J. Mech. Behav. Biomed. Mater.* **2016**, *59*, 128–138. [CrossRef] [PubMed]
32. Kanchanavasita, W.; Triwatana, P.; Suputtamongkol, K.; Thanapitak, A.; Chatchaiganan, M. Contrast ratio of six zirconia-based dental ceramics. *J. Prosthodont.* **2014**, *23*, 456–461. [CrossRef] [PubMed]
33. Shahmiri, R.; Standard, O.C.; Hart, J.N.; Sorrell, C.C. Optical properties of zirconia ceramics for esthetic dental restorations: A systematic review. *J. Prosthet. Dent.* **2018**, *119*, 36–46. [CrossRef] [PubMed]
34. Yamashita, I.; Tsukuma, K. Light scattering by residual pores in transparent zirconia ceramics. *J. Ceram. Soc. Jpn.* **2011**, *119*, 133–135. [CrossRef]
35. Kim, H.K.; Kim, S.H.; Lee, J.B.; Ha, S.R. Effects of surface treatments on the translucency, opalescence, and surface texture of dental monolithic zirconia ceramics. *J. Prosthet. Dent.* **2016**, *115*, 773–779. [CrossRef] [PubMed]
36. Jiang, L.; Liao, Y.; Wan, Q.; Li, W. Effects of sintering temperature and particle size on the translucency of zirconium dioxide dental ceramic. *J. Mater. Sci. Mater. Med.* **2011**, *22*, 2429–2435. [CrossRef] [PubMed]
37. Zhang, H.; Kim, B.N.; Morita, K.; Keijiro Hiraga, H.Y.; Sakka, Y. Effect of sintering temperature on optical properties and microstructure of translucent zirconia prepared by high-pressure spark plasma sintering. *Sci. Technol. Adv. Mater.* **2011**, *12*, 055003. [CrossRef] [PubMed]
38. Papageorgiou-Kyrana, K.; Fasoula, M.; Kontonasaki, E. Translucency of Monolithic Zirconia after Hydrothermal Aging: A Review of In Vitro Studies. *J. Prosthodont.* **2020**, *29*, 489–500. [CrossRef] [PubMed]
39. Hajhamid, B.; Alfrisany, N.; Somogyi-Ganss, E. The effect of accelerated aging on crystalline structures and optical properties of different monolithic zirconia: A qualitative systematic review. *Dent. Mater.* **2022**, *38*, 569–586. [CrossRef] [PubMed]
40. Abdelbary, O.; Wahsh, M.; Sherif, A.; Salah, T. Effect of accelerated aging on translucency of monolithic zirconia. *Future Dent. J.* **2016**, *2*, 65–69. [CrossRef]
41. Walczak, K.; Meißner, H.; Range, U.; Sakkas, A.; Boening, K.; Wieckiewicz, M.; Konstantinidis, I. Translucency of Zirconia Ceramics before and after Artificial Aging. *J. Prosthodont.* **2019**, *28*, e319–e324. [CrossRef] [PubMed]
42. Zhang, C.Y.; Agingu, C.; Tsoi, J.K.H.; Yu, H. Effects of Aging on the Color and Translucency of Monolithic Translucent Y-TZP Ceramics: A Systematic Review and Meta-Analysis of In Vitro Studies. *BioMed Res. Int.* **2021**, *2021*, 8875023. [CrossRef] [PubMed]
43. Zhang, F.; Vanmeensel, K.; Inokoshi, M.; Batuk, M.; Hadermann, J.; Van Meerbeek, B.; Naert, I.; Vleugels, J. 3Y-TZP ceramics with improved hydrothermal degradation resistance and fracture toughness. *J. Eur. Ceram. Soc.* **2014**, *34*, 2453–2463. [CrossRef]
44. Nogiwa-Valdez, A.A.; Rainforth, W.M.; Zeng, P.; Ross, I.M. Deceleration of hydrothermal degradation of 3Y-TZP by alumina and lanthana co-doping. *Acta Biomater.* **2013**, *9*, 6226–6235. [CrossRef] [PubMed]
45. Zhang, Y. Making yttria-stabilized tetragonal zirconia translucent. *Dent. Mater.* **2014**, *30*, 1195–1203. [CrossRef] [PubMed]
46. Stawarczyk, B.; Emslander, A.; Roos, M.; Sener, B.; Noack, F.; Keul, C. Zirconia ceramics, their contrast ratio and grain size depending on sintering parameters. *Dent. Mater. J.* **2014**, *33*, 591–598. [CrossRef] [PubMed]
47. Zhang, F.; Vanmeensel, K.; Batuk, M.; Hadermann, J.; Inokoshi, M.; Van Meerbeek, B.; Naert, I.; Vleugels, J. Highly-translucent, strong and aging-resistant 3Y-TZP ceramics for dental restoration by grain boundary segregation. *Acta Biomater.* **2015**, *16*, 215–222. [CrossRef] [PubMed]
48. Pekkan, G.; Pekkan, K.; Bayindir, B.; Özcan, M.; Karasu, B. Factors affecting the translucency of monolithic zirconia ceramics: A review from materials science perspective. *Dent. Mater. J.* **2020**, *39*, 1–8. [CrossRef] [PubMed]
49. Alghazzawi, T.F. The effect of extended aging on the optical properties of different zirconia materials. *J. Prosthodont. Res.* **2017**, *61*, 305–314. [CrossRef] [PubMed]

50. Pereira, G.K.R.; Venturini, A.B.; Silvestri, T.; Dapieve, K.S.; Montagner, A.F.; Soares, F.Z.M.; Valandro, L.F. Low-temperature degradation of Y-TZP ceramics: A systematic review and meta-analysis. *J. Mech. Behav. Biomed. Mater.* **2015**, *55*, 151–163. [CrossRef] [PubMed]
51. Pereira, G.K.R.; Muller, C.; Wandscher, V.F.; Rippe, M.P.; Kleverlaan, C.J.; Valandro, L.F. Comparison of different low-temperature aging protocols: Its effects on the mechanical behavior of Y-TZP ceramics. *J. Mech. Behav. Biomed. Mater.* **2016**, *60*, 324–330. [CrossRef] [PubMed]
52. de Araújo-Júnior, E.N.S.; Bergamo, E.T.P.; Campos, T.M.B.; Benalcázar Jalkh, E.B.; Lopes, A.C.O.; Monteiro, K.N.; Cesar, P.F.; Tognolo, F.C.; Tanaka, R.; Bonfante, E.A. Hydrothermal degradation methods affect the properties and phase transformation depth of translucent zirconia. *J. Mech. Behav. Biomed. Mater.* **2020**, *112*, 104021. [CrossRef] [PubMed]
53. Kim, J.W.; Covel, N.S.; Guess, P.C.; Rekow, E.D.; Zhang, Y. Concerns of hydrothermal degradation in CAD/CAM zirconia. *J. Dent. Res.* **2010**, *89*, 91–95. [CrossRef] [PubMed]
54. Flinn, B.D.; Raigrodski, A.J.; Singh, A.; Mancl, L.A. Effect of hydrothermal degradation on three types of zirconias for dental application. *J. Prosthet. Dent.* **2014**, *112*, 1377–1384. [CrossRef] [PubMed]
55. Flinn, B.D.; Raigrodski, A.J.; Mancl, L.A.; Toivola, R.; Kuykendall, T. Influence of aging on flexural strength of translucent zirconia for monolithic restorations. *J. Prosthet. Dent.* **2017**, *117*, 303–309. [CrossRef] [PubMed]
56. Zhang, Y.; Lawn, B.R. Novel Zirconia Materials in Dentistry. *J. Dent. Res.* **2018**, *97*, 140–147. [CrossRef] [PubMed]
57. Fathy, S.M.; El-Fallal, A.A.; El-Negoly, S.A.; El Bedawy, A.B. Translucency of monolithic and core zirconia after hydrothermal aging. *Acta Biomater. Odontol. Scand.* **2015**, *1*, 86–92. [CrossRef] [PubMed]
58. Kim, H.K.; Kim, S.H. Effect of hydrothermal aging on the optical properties of precolored dental monolithic zirconia ceramics. *J. Prosthet. Dent.* **2019**, *121*, 676–682. [CrossRef] [PubMed]
59. Choi, Y.S.; Kang, K.H.; Att, W. Effect of aging process on some properties of conventional and multilayered translucent zirconia for monolithic restorations. *Ceram. Int.* **2020**, *46*, 1854–1868. [CrossRef]
60. Klimke, J.; Trunec, M.; Krell, A. Transparent tetragonal yttria-stabilized zirconia ceramics: Influence of scattering caused by birefringence. *J. Am. Ceram. Soc.* **2011**, *94*, 1850–1858. [CrossRef]
61. Wang, J.; Rainforth, M.; Stevens, R. The grain size dependence of the mechanical properties in TZP ceramics. In *Zirconia'88ed*; Springer: Berlin/Heidelberg, Germany, 1989; pp. 337–366.
62. Camposilvan, E.; Leone, R.; Gremillard, L.; Sorrentino, R.; Zarone, F.; Ferrari, M.; Chevalier, J. Aging resistance, mechanical properties and translucency of different yttria-stabilized zirconia ceramics for monolithic dental crown applications. *Dent. Mater.* **2018**, *34*, 879–890. [CrossRef] [PubMed]
63. Guilardi, L.F.; Pereira, G.K.R.; Gündel, A.; Rippe, M.P.; Valandro, L.F. Surface micro-morphology, phase transformation, and mechanical reliability of ground and aged monolithic zirconia ceramic. *J. Mech. Behav. Biomed. Mater.* **2017**, *65*, 849–856. [CrossRef] [PubMed]
64. Hatanaka, G.R.; Polli, G.S.; Adabo, G.L. The mechanical behavior of high-translucent monolithic zirconia after adjustment and finishing procedures and artificial aging. *J. Prosthet. Dent.* **2020**, *123*, 330–337. [CrossRef] [PubMed]
65. Amat, N.F.; Muchtar, A.; Amril, M.S.; Ghazali, M.J.; Yahaya, N. Effect of sintering temperature on the aging resistance and mechanical properties of monolithic zirconia. *J. Mater. Res. Technol.* **2019**, *8*, 1092–1101. [CrossRef]
66. Borchers, L.; Stiesch, M.; Bach, F.W.; Buhl, J.C.; Hübsch, C.; Kellner, T.; Kohorst, P.; Jendras, M. Influence of hydrothermal and mechanical conditions on the strength of zirconia. *Acta Biomater.* **2010**, *6*, 4547–4552. [CrossRef] [PubMed]
67. Alghazzawi, T.F.; Lemons, J.; Liu, P.R.; Essig, M.E.; Bartolucci, A.A.; Janowski, G.M. Influence of low-temperature environmental exposure on the mechanical properties and structural stability of dental zirconia. *J. Prosthodont.* **2012**, *21*, 363–369. [CrossRef] [PubMed]
68. Siarampi, E.; Kontonasaki, E.; Andrikopoulos, K.S.; Kantiranis, N.; Voyiatzis, G.A.; Zorba, T.; Paraskevopoulos, K.M.; Koidis, P. Effect of in vitro aging on the flexural strength and probability to fracture of Y-TZP zirconia ceramics for all-ceramic restorations. *Dent. Mater.* **2014**, *30*, e306–316. [CrossRef] [PubMed]
69. Kim, H.T.; Han, J.S.; Yang, J.H.; Lee, J.B.; Kim, S.H. The effect of low temperature aging on the mechanical property & phase stability of Y-TZP ceramics. *J. Adv. Prosthodont.* **2009**, *1*, 113–117. [CrossRef] [PubMed]
70. Inokoshi, M.; Vanmeensel, K.; Zhang, F.; De Munck, J.; Eliades, G.; Minakuchi, S.; Naert, I.; Van Meerbeek, B.; Vleugels, J. Aging resistance of surface-treated dental zirconia. *Dent. Mater.* **2015**, *31*, 182–194. [CrossRef] [PubMed]
71. Chevalier, J.; Cales, B.; Drouin, J.M. Low-temperature aging of Y-TZP ceramics. *J. Am. Ceram. Soc.* **1999**, *82*, 2150–2154. [CrossRef]

Disclaimer/Publisher's Note: The statements, opinions and data contained in all publications are solely those of the individual author(s) and contributor(s) and not of MDPI and/or the editor(s). MDPI and/or the editor(s) disclaim responsibility for any injury to people or property resulting from any ideas, methods, instructions or products referred to in the content.